

Visualization of cross sectional data for morphogenetic studies

G. Brunnett, M. Vančo, Ch. Haller, S. Washausen, H.-J. Kuhn, W. Knabe

Abstract: We report on a visualization system that has been implemented to study cellular events which regulate morphogenesis of large organs or whole embryos. For data acquisition the recently established system “Huge Image ” is employed. Each resulting image of an entire histological section is loaded into AutoCAD for manual contour creation and cytological diagnosis. In a subsequent step an automatic procedure detects and repairs contour artifacts in order to provide clean contour data. A modified version of Boissonnat’s reconstruction algorithm is used to create 3D models from contour data. The user is allowed to choose from different modes for appropriate visualization of surfaces and data resulting from cytological diagnosis.

1 Introduction

Three-dimensional reconstructions have provided valuable new information in many fields of biological research. This holds especially true for developmental biology. Here, comprehensive visualization of changes in the shape of complex biological objects is a prerequisite to understand the morphogenesis of organs or entire embryos. In the beginning, three-dimensional reconstructions were carried out by building up physical models of the outer surface of serially sectioned biological objects. More recent advances in cellular and molecular biology have contributed an ever increasing number of data on cellular events which regulate morphogenesis. Consequently, improved visualization techniques are needed to evaluate how distinct morphogenetic steps are correlated with a multitude of simultaneously or sequentially occurring cellular and molecular events. Refined three-dimensional reconstruction techniques, among other approaches, will play a central role in these projects.

The present work briefly describes a recently established system for the visualization of 3D reconstructions of biological objects combined with data resulting from cytological diagnosis in histological sections. Emphasis will be given to the acquisition, processing and correction of vectorized contour data as well as to surface generation with the help of triangulation algorithms.

For data acquisition we use a system “Huge Image” [Su02, Kn02]. This scanning device is used to provide high resolution images of entire histological sections. These images are loaded into AutoCAD for manual contour creation and cytological diagnosis. The resulting data is forwarded to our reconstruction module. Our reconstruction method is a modified version of Boissonnat’s approach [Bois88]. Since our implementation of Boissonnat’s approach showed unexpected defects in the reconstruction, we replaced the tetrahedra removal by an incremental surface construction technique.

2 Data acquisition

Figure 1 demonstrates how vectorized contour data are acquired from intact biological objects. Details of the embryos and of the preparation procedures used are specified in [KSK00]. Resin-embedded embryos are completely serially sectioned at $1\mu\text{m}$ section thickness. To visualize surfaces and cellular details of the object, histological serial sections are routinely stained with hematoxylin/Heidenhain [Ro89]. For image acquisition, stained sections are scanned with “Huge Image” [Su02, Kn02]. Major components of this scanning system are a digital camera (Axiocam HR, Zeiss, Göttingen, Germany), a light microscope with motorized z-drive (Axioskop 2 MOT, Zeiss) and a motorized scanning table (Märzhäuser, Wetzlar, Germany), all connected to a PC. This PC is run with Windows 2000 (Microsoft, Berlin, Germany), with MosaiX (KS400 Zeiss) for image acquisition, and is equipped with two 350 MHz CPUs, 50 GB hard disk memory, and 640 MB working memory. “Huge Image” permits scanning at variable resolutions. Thus, the degree of object detail required and the expense of time needed for scanning can be adjusted for a broad range of biological applications. Different from other systems, scanning is also feasible with maximum resolution of the light microscope [Su02, Kn02]. Small scanned images from all single fields of view of the camera are automatically assembled to one “huge image” of the entire histological section. In KS400 (Zeiss) the scanning procedure can be individually modified by macros. We have implemented free adjustment of the number of slides, the number of scanned sections on each slide, the scanned area of each section, the autofocus device, and the blank field correction [Su02]. With the help of graphics tablets (Intuous A3, Wacom, Krefeld, Germany), contours of the biological object are manually vectorized (Fig. 1) in AutoCAD 2000i (Autodesk GmbH, München, Germany). In biological objects, contours of interest are often penetrated by other contours, e.g. vessels which invade the brain. Consequently, commercially available programs for automatized contour recognition could not be successfully applied. Following vectorization, supernumerary vertices of the contour lines which, in part, resulted from automatized joining of individually drawn segments of the contours were weeded with Polyline specialist 2.04 (Four Dimension Technologies, Bangalore, India). Next, vectorized sections are realigned predominantly by external fiducials [Kn02]. It is important to note that the AutoCAD data exported to the visualization system is organized to the different surfaces, i.e. each exported file contains only contours belonging to the same surface of the object.

During the manual contour creation several types of errors and problems can be introduced into the data by the human operator. Since our reconstruction program is sensitive to certain point configurations we found it necessary to implement a preprocessing procedure that detects and removes these special cases.

3 Surface reconstruction

After application of the cleaning procedure the data can be used as input for our reconstruction algorithm that is a modified version of Boissonnat’s approach [Bois88].

The original method of Boissonnat consists of three major steps. Initially, the Delaunay tetrahedralization of the given data set is computed. In the second step certain tetrahedra are

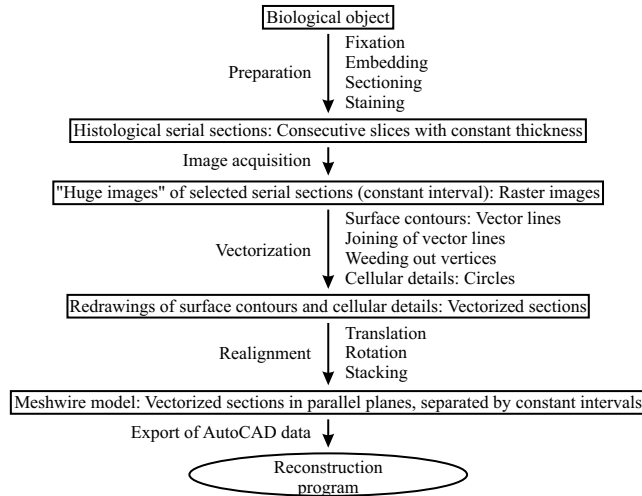


Abbildung 1: Acquisition of contour data from biological objects

removed from the convex hull to create a volumetric reconstruction of the original object. Finally, the boundary triangles are extracted from the tetrahedra set to obtain a description of the object's boundary. Our method modifies this approach by substituting the steps of tetrahedra removal and surface extraction by an incremental surface construction technique that is performed on the triangles of the complete tetrahedra set.

In the case of reconstruction from contours all data points lie in parallel planes. It has been shown in [Bois88] that in this situation the Delaunay tetrahedralization can be computed efficiently based on the Delaunay triangulations of the contours in the sections. However, it is not guaranteed that the Delaunay triangulation of the vertex set of a contour contains all contour edges. If some contour edges are not present in the Delaunay triangulation, additional points on these edges have to be inserted into the data set.

The dual graph of the Delaunay triangulation is the *Voronoi diagram*, see e.g. [Rou98] for basic definitions.

For the Voronoi diagram of the vertex set of contour lines one can define the following important subgraphs. The *internal Voronoi skeleton (IVS)* is formed by those Voronoi edges that are dual to Delaunay edges which lie in the interior of a contour. In the same way the *external Voronoi skeleton (EVS)* consists of those Voronoi edges dual to Delaunay edges in the exterior of any contour (see fig. 2 a)).

If the points density is sufficiently high, the external Voronoi skeleton separates different contours and concavities of non-convex contours. The quality of the reconstruction can be improved by inserting additional points into one section that are projections of points from the EVS of a neighboring slice, see fig. 2 b)).

From the triangulations of two neighboring sections S_1 and S_2 the Delaunay tetrahedralization can be obtained by constructing three different types of tetrahedra. The first type, $T1$ tetrahedra (fig. 3 a)) is obtained in the following way: let \mathcal{T} denote a triangle in the lower contour S_1 and V be the Voronoi vertex dual to \mathcal{T} . Then V is orthogonally projected onto

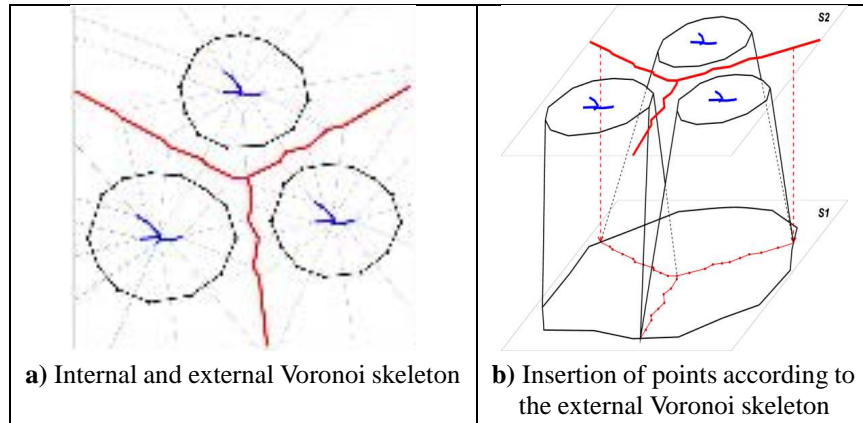


Abbildung 2: Voronoi skeletons

S_2 and the closest data point P in S_2 to this projection is determined. The tetrahedron T_1 is formed by the vertices of \mathcal{T} and P .

The T_2 tetrahedra (fig. 3 **b**) are formed in the analogous way by joining a triangle \mathcal{T} in S_2 with a point in S_1 that is closest to the projection of the Voronoi vertex dual to \mathcal{T} . A tetrahedron of type T_{12} is formed from vertices of a Delaunay edge in S_1 and a Delaunay edge in S_2 . The criterion for merging two Delaunay edges into one T_{12} tetrahedron is an intersection of the dual Voronoi edges orthogonally projected to one section (fig. 3 **c**). In the fig. (fig. 3 **d**) the complete tetrahedralization of one layer is shown.

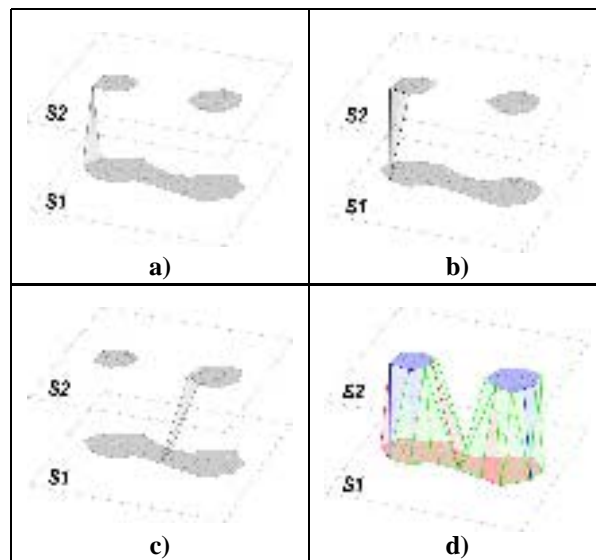


Abbildung 3: Tetrahedralization: **a**) T_1 tetrahedra, **b**) T_2 tetrahedra, **c**) T_{12} tetrahedra, **d**) complete tetrahedralization (with subsequent elimination)

For the sculpturing process Boissonnat has formulated a set of criteria for the removal of tetrahedra from the convex hull. However, we observed that several undesirable tetrahedra configurations may occur for which no removal criterion has been formulated. In fig. 4 one of these cases is illustrated that we refer to as a ‘boundary fold-over’. This case can be easily detected (there are some contour edges with 4 incident triangles), but it is difficult to determine automatically, which tetrahedra have to be removed.

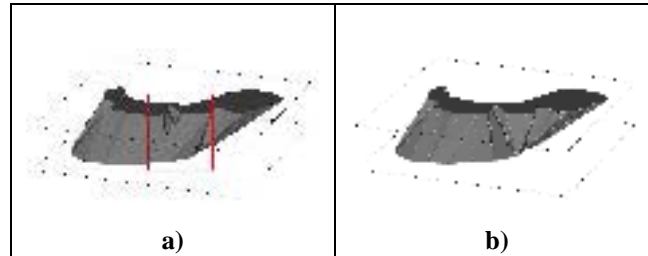


Abbildung 4: Defects on the object's surface

Therefore we developed a new procedure that directly constructs a surface from the tetrahedralization. Since we enforce that each edge of the triangulation is incident only to two triangles, unwanted cases as boundary fold-overs are avoided.

At first the tetrahedra neighborhood information (data structure) for all layers have to be created. Then the procedure takes one layer and creates a list of candidate triangles for which we assume the position on the object's surface. For complicated surfaces with many concavities only a few triangles are on the object's surface (the remaining ones lie “under” tetrahedra which have to be removed). The probability that we choose a wrong triangle is high and if the surface creation process fails, the procedure should be able to take the next triangle from the candidate list and repeat the searching.

The tetrahedra parsing is illustrated in the fig. 5: the bottom right image shows the correct surface which should be extracted from the tetrahedralized surface shown on the left images. Two parsing steps after the starting triangle the procedure detects an edge e with two triangle neighbors. The procedure saves this ambiguous edge e into a stack, chooses one triangle neighbor and continues parsing. During parsing all visited contour edges are marked. After two next steps of parsing the path 1 (upper image) the procedure detects that the path would return on a marked contour edge (upper contour - the rear side of the black tetrahedron). This contradicts to our definition of a correct surface and therefore the path 1 is deleted, the procedure pops from the stack the edge e and chooses the path 2 (bottom image), which creates a correct object's surface.

Fig. 6 shows reconstructions computed with the described method. The system can visualize any number of surfaces and offers a large variety of visualization options as color, lights, transparency, depth cueing, motion, animation etc.

Acknowledgements: This work was supported by grants BR 1185/4-1 (4-2) and KN 525/1-1, 1-2 of the Deutsche Forschungsgemeinschaft (DFG).

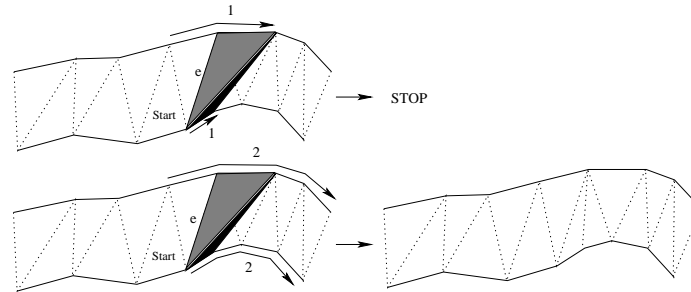


Abbildung 5: Parsing the tetrahedra

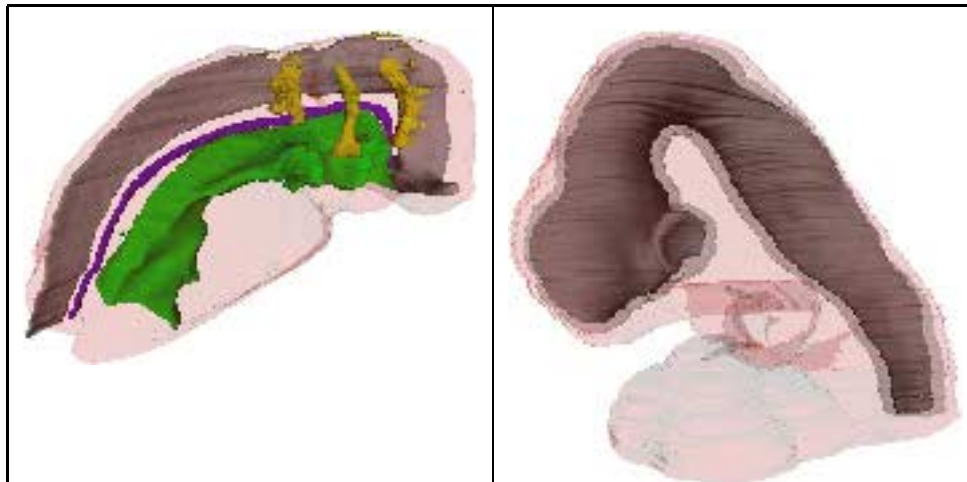


Abbildung 6: Reconstruction results

Literatur

- [Bois88] **Boissonnat, J.:** Shape reconstruction from planar cross-sections, *Computer Vision, Graphics, and Image Processing*, 44(1): 1–29, Oct. 1988.
- [KSK00] **Knabe, W.; Süß, M.; Kuhn, H.-J.:** The patterns of cell death and of macrophages in the developing forebrain of the tree shrew *Tupaia belangeri*, *Anatomy and Embryology*, 2000; 201; pp. 157–168.
- [Kn02] **Knabe, W.; Washausen, S.; Brunnett, G.; Kuhn, H.-J.:** Use of “reference series” to realign histological serial sections for three-dimensional reconstructions of the positions of cellular events in the developing brain, *Journal of Neuroscience Methods*, 2002; 121; pp. 169–180.
- [Rou98] **O’Rourke:** Computational Geometry in C, *Cambridge University Press*, September 1998.
- [Ro89] **Romeis, B.:** Mikroskopische Technik, (Böck, P.; Ed.). *Urban and Schwarzenberg*, München/Wien, 1989; p. 219.
- [Su02] **Süß, M.; Washausen, S.; Kuhn, H.-J.; Knabe, W.:** High resolution scanning and three-dimensional reconstruction of cellular events in large objects during brain development, *Journal of Neuroscience Methods*, 2002; 113; pp. 147–158.